

# Atomistic modeling and physical comprehension of the effects of implant dose rate on boron activation in pMOSFET S/D

J. Singer, F. Salvetti, V. Kaepelin  
NXP Semiconductors  
38926 Crolles, France

M. Jaraiz, P. Castrillo, E. Rubio  
University of Valladolid  
47011 Valladolid, Spain

F. Wacquant, N. Cagnat  
STMicroelectronics  
38926 Crolles, France

A. Poncet  
Lyon Nanotechnologies Institute  
(UMR-CNRS 5270)  
69621 Villeurbanne, France

**Abstract**—This study is aimed to understand the mechanisms leading to different device behaviors while switching from one type of implanter, which scans a batch of wafers with a spot ion beam, to another one, which scans a single wafer with a ribbon ion beam. Thanks to atomistic simulations, we bring to the fore that the implant dose rate is responsible for the observed mismatch. Increasing the dose rate reduces the amount of interstitials present beyond the amorphous layer. During subsequent annealing, these interstitials first accelerate boron clusters dissolution at projected range, then agglomerate themselves into stable dislocation loops. The latter will in turn deactivate the boron in source and drain region, modifying the electrical characteristics of the device.

## I. INTRODUCTION

MOSFETs undergo size reduction according to Moore's law from about half a century. Following gate length scaling, junction depth has to be drastically reduced while contact resistances have to be kept low enough in order to preserve the device performance. With high temperature fast anneals following ion implantation steps, conditions of junction formation are kept far from equilibrium. In particular, boron (B) diffusion and activation are driven by self-interstitial (I) supersaturation during the process, which in turn strongly depends on the presence of small clusters and extended defects ( $\{311\}$  defects and dislocation loops, noted DLoops afterwards).

Thus generation of defects during implant plays a crucial role in the future device characteristics. In addition to the dose and energy of implantation, it has become important to manage the dose rate (DR), as this parameter has an impact on defect accumulation during implant [1, 2]. In particular switching from batch tool with spot ion beam toward single-wafer tool with ribbon ion beam can lead to different device behavior because the effective DR are in principle different. In order to match device characteristics for both tools it is crucial to understand the causes of these differences.

This study is aimed to understand the mechanisms responsible for different junction behavior with same implant parameters, apart from the DR. Atomistic simulations of B clustering under different conditions are performed in order to evidence these mechanisms.

## II. METHOD AND EXPERIMENTS

Typical source and drain (S/D) implants on MOSFET devices were performed in order to compare two types of implanters. The first one is characterized by a spot ion beam, screening a batch of 13 wafers ; the other one scans a single wafer with a ribbon beam, as long as 300mm.

To better understand junction behavior on devices, similar junctions were fabricated on blanket wafers, allowing secondary ion mass spectroscopy (SIMS) analysis. A S/D-type  $\text{BF}_2$  implantation at an energy of 15 keV and a dose of  $3.6\text{E}15\text{cm}^{-2}$  was performed either with the batch or with the single-wafer implanter, followed for all samples by an implant of B at 13 keV,  $6\text{E}13\text{cm}^{-2}$ . Spike anneal at  $1113^\circ\text{C}$  was then performed to compare electrical characteristics with devices. More experimental details can be found in [1].

We used DADOS, a software developed by the University of Valladolid, to perform atomistic simulations [3]. The strength of this kind of simulator is its ability to help the user understand the physics behind unexpected behaviors.

## III. RESULTS AND DISCUSSION

### A. Device mismatch

It was first observed that switching from spot beam to ribbon beam implanter lead to a lower sheet resistance ( $R_s$ ) of the active layer of 6%, well above the measurement error. As mentioned in [4], this change in  $R_s$  could not be explained by an eventual dose shift between both implanters, since all classical parameters were matched before.

## B. Atomistic simulations and full sheet experiments

### 1) B clustering evolution at projected range

We performed atomistic simulations in order to understand the differences experimentally observed. The idea is to look at B clusters evolution.

To facilitate interpretation of simulations and favor physical comprehension instead of experiment fitting, we first use the very simple structures described on Fig. 1, with square-shaped profiles of B and interstitials. However it is essential to respect the following details so as to interpret the B profile evolution, and afterwards linking simulation to experiments.

Designed from the as-implanted profile, the square-shaped B profile was 10 nm-wide, with a concentration similar to the maximum one of the B as-implanted profile; and located at the implant projected range ( $R_p$ ). Since the  $BF_2$  implant amorphizes the substrate we also put an amorphous layer in our structure. Indeed if no amorphous layer is introduced all B will be active, but during solid phase epitaxial regrowth (SPER) B atoms are shared between active (potentially mobile) and clustered B (immobile). In addition we cannot neglect interstitials and vacancies trapping by amorphous/crystalline (a/c) interface before complete recrystallization. A square-shaped profile of interstitials was used, with a concentration varying from  $1E20$  to  $5E21$   $cm^{-3}$ . Its position corresponds to the highly damaged region, called end of range (EoR) region. Since no defects are left in the recrystallized layer after annealing we do not include interstitials in the amorphous layer. The width of 5 nm is close to the interstitials peak found just behind a/c after implant. The temperature profile of the anneal is also respected, especially at high temperature.

Initially no DLoops will be formed in the simulation, in order to dissociate the different effects and draw reliable conclusions.

Annealing of this simple structure leads to the following conclusion: increasing the amount of interstitials at EoR location favors boron-interstitial clusters (BICs) dissolution at  $R_p$ . In this simulation, as no extended defects are present, B atoms which escaped from BICs undergo diffusion. Thus the diffusion tail is longer when more BICs dissolved. B profile evolution is shown on Fig. 2.

Atomistic mechanism of BICs dissolution is the following. After recrystallization most of BICs are in the form of  $B_3I$  and  $B_2$ , where I corresponds to 'interstitial'. In their presence three mechanisms dominate:

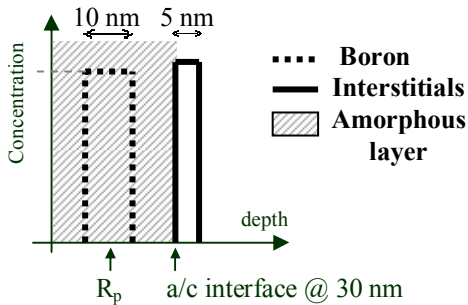


Figure 1. Description of the simple structure used for atomistic simulations.

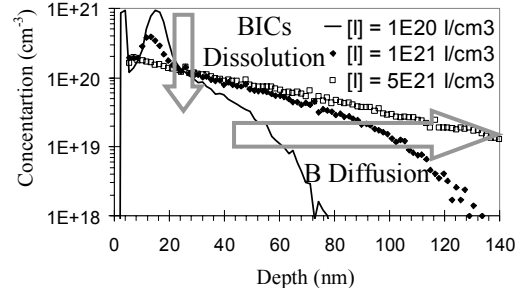


Figure 2. Square-shaped B profile evolution after annealing with different amounts of EoR-located interstitials.



$B_3I$  can emit a mobile B atom (1) paired off with an interstitial (BI). Thus at the beginning of annealing  $B_2$  comes either from SPER deposition and/or from  $B_3I$  dissolution. What  $B_2$  will capture will determine the future evolution of BICs. If a  $B_2$  captures a pair BI (2) to form again  $B_3I$ , the clusters evolve toward stabilization. If  $B_2$  captures an interstitial (3)  $B_2I$  is formed, which is very unstable. It will very quickly dissolve by emitting a BI itself and leaving behind an active, substitutional  $B_s$  atom. Thus when the concentration of interstitials at EoR is high enough, the capture of an interstitial by  $B_2$  becomes more probable than the capture of a BI. Reaction (3) becomes dominant. That's why the BICs dissolution is favored when the interstitial concentration increases.

However the way by which we increased the amount of interstitials is here quite artificial; instead of that, one can vary it by modifying the amorphous depth. Indeed, on the one hand all defects (both Frenkel pairs and interstitials in excess) that are in an amorphized region will be annihilated during recrystallization; on the other hand the interstitial profile given by the "+I model" [5, 6] (i.e. the interstitials which will not recombine with vacancies) is determined when the energy, dose and tilt angle are fixed. Thus varying the amorphous depth while keeping constant the implant dose, energy, and tilt angle, will change the amount of interstitials in excess present at EoR region, as illustrated on Fig. 3.

With the next simulation we try to look at B clustering at  $R_p$  using as-implanted B profile as dopant and varying amorphous depth. We also use interstitials and vacancies as-implanted profiles, generated by a Monte Carlo implant simulator (UT Marlowe), that will give the right interstitials net profile. The structure is presented on Fig. 4.

As a result, we effectively obtain after spike anneal 15% less B in BICs with an amorphous layer narrower of 2.5 nm. B mainly clusters

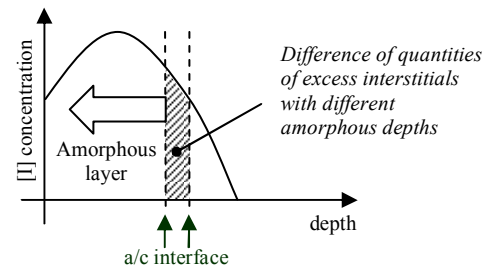


Figure 3. Schematic illustration of the variation of excess interstitials amount by means of amorphous depth variation. Interstitials in excess disappear in the amorphous region during SPER.

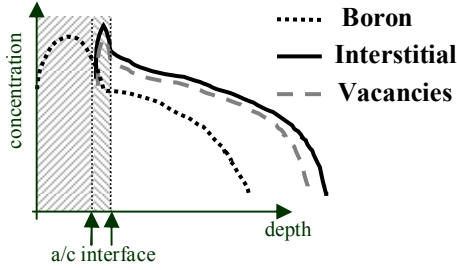


Figure 4. Description of the more realistic structure used for atomistic simulations.

at  $R_p$  because this is the region with highest B concentration [7]. The profiles of clustered B are given in Fig. 5.

This simulation shows that little variation in amorphous depth can lead to a significant difference of B clustering at  $R_p$ .

But how can we justify a change in amorphous depth between two implants if the energy, dose, and tilt angle are kept constant? Amorphization of silicon lattice is obtained by accumulation of interstitials/vacancies (I/V) Frenkel pairs during implant [6]. If we give in average more (resp. less) time between each ion collision, we will increase (resp. decrease) the efficiency of I/V pairs recombination during implant. One solution thus is to change the implant dose rate (DR). This parameter represents the implantation velocity, and is calculated as follows:

$$DR = \frac{\text{Dose}}{\text{ImplantationTime} \times \text{NumberOfWafers}} \quad [1]. \quad (4)$$

The DR is measured in atoms per centimeter square per second ( $\text{at.cm}^{-2}.\text{s}^{-1}$ ). Increasing the DR is a way to reduce the time between two collisions, allowing more damage accumulation. Consequently a higher DR should result in a deeper amorphous layer for similar implants. This has effectively been observed in the experiments of Cagnat and co-workers [1] and is plotted on Fig. 6.

Although the direct measurement of interstitials amount after implant is not possible, it is directly linked to the number and to the size of DLoops. So they noted moreover that the excess amount of interstitials present at EoR after implant decreased as the amorphous depth increased (together with the dose rate), as-expected (Fig. 7).

## 2) Boron accumulation and deactivation at end of range

More numerous and more stable DLoops are formed when the DR is decreased. But DLoops are known to trap B (accumulation) and to deactivate it [8]. In our case, DLoops trap both (i) the B escaped from BICs dissolution at  $R_p$  and (ii) some of the active B

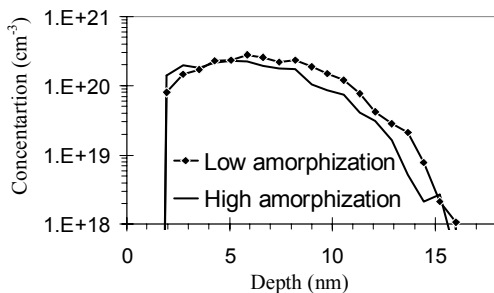


Figure 5. Profiles of clustered B at  $R_p$  after anneal for two different amorphous depths.

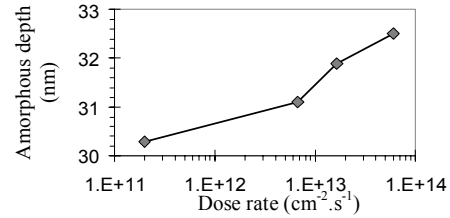


Figure 6. Amorphous depth as a function of implant dose rate. Experimental data from [1].

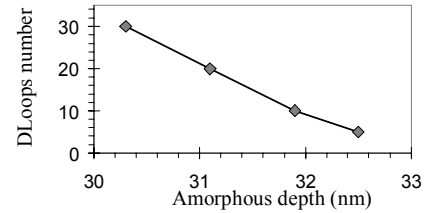


Figure 7. Number of DLoops (representative of interstitial content) observed as a function of the amorphous depth. Experimental data from [1].

located around them.

This explains SIMS analyses of Fig. 8 made on full sheet implants, followed by the same spike anneal than on devices.

(i) Following our previous demonstration, we expect that a high DR would favor B accumulation at  $R_p$ , because the amount of interstitials present at EoR is lower. On the other side a low DR should favor B accumulation near EoR region, to the detriment of B accumulation at  $R_p$ .

Indeed after spike anneal B showed a clear trend to accumulate either at  $R_p$  with a high DR (deeper amorphous layer) or at EoR with a low DR (narrower amorphous depth).

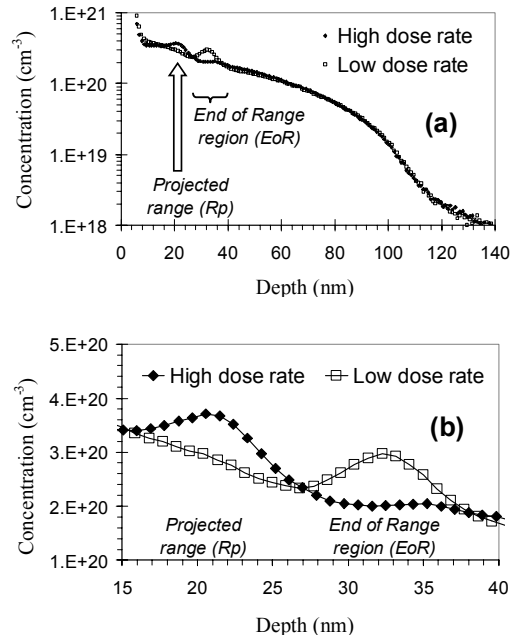


Figure 8. Experimental SIMS profiles of spike-annealed B for two different dose rates (a) from [1]. Zoom on the two bumps (b).

We can observe on Fig. 9 that the sum of the B doses present in the two bumps is almost constant whatever the amorphous depth. This is the experimental evidence that B atoms emitted from BICs at  $R_p$  are captured by DLoops when present.

(ii) Moreover DLoops tend to deactivate B gravitating around EoR region. This can be seen by a detailed comparison of SIMS profiles near EoR region. As shown before, when amorphous depth is less important, less clustering at  $R_p$  is obtained; however not all B atoms released from clusters are active. On the contrary, EoR-located DLoops capture (and deactivate) these B atoms liberated from BICs at  $R_p$ , but also mobile B atoms going through EoR barrier. The latter B atoms were active (i.e. in substitutional site), thus potentially mobile by kick-out mechanism [9]; during their migration steps they were captured by DLoops.

This is observable on the SIMS profile by a slight B desertion in the region surrounding EoR region, which is pointed out on the Fig. 10. If one extrapolates this part of the profile to get the active B concentration (not shown), the  $R_s$  variation between both is around 4%, to be compared with the 6% found on devices.

This explains why the  $R_s$  of the active layer increases when there are more interstitials left at EoR after SPER, even if BICs situated at  $R_p$  dissolve faster. A lower DR, which amorphizes less and leaves stable extended defects at EoR, leads to a higher  $R_s$ .

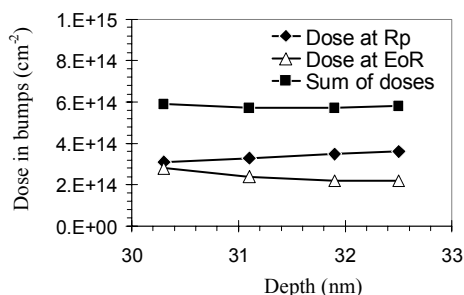


Figure 9. B doses in each bump and their sum as a function of amorphous depth.

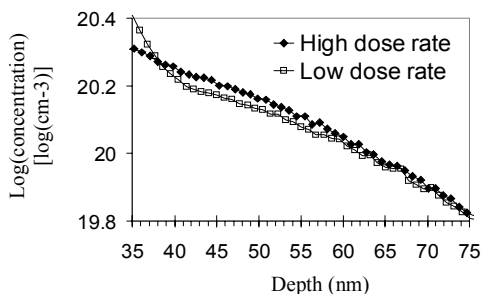


Figure 10. Zoom near EoR region on the SIMS B profiles of Fig. 8.

#### IV. CONCLUSION

In this paper we investigated the atomistic mechanisms responsible for the effect of implanter type on device characteristics. It was found that the dose rate is responsible for the potential device mismatch observation between both implanters. A lower DR leads to a narrower amorphous layer, which in turn leaves more interstitials in excess behind a/c interface. Atomistic simulations were used to bring out that these interstitials were directly responsible for the more rapid BICs dissolution at  $R_p$ . In addition they formed more numerous and more stable dislocation loops which are able to capture not only B atoms coming from BICs dissolution at  $R_p$  but also active B close to EoR region. The dose rate varying from batch tool to single-wafer tool from  $2E11$  to  $6E13 \text{ at.cm}^{-2}.s^{-1}$ , respectively [1], this explains thus the lowering of  $R_s$  observed on pMOSFET device when DR is increased, while switching from the first equipment to the second one.

#### REFERENCES

- [1] N. Cagnat, C. Laviron, N. Auriac, J. Liu, S. Mehta et al., "Defect behavior in  $BF_2$  implants for S/D applications as a function of ion beam characteristics", Ion Impl. Tech. Conf. Proc., vol. 866, pp. 133-136, 2006.
- [2] L. Pelaz, G. H. Gilmer, V. C. Venezia, H.-J. Gossmann, M. Jaraiz, J. Barbolla, "Modeling of the effects of the dose, dose rate, and implant temperature on transient enhanced diffusion", Appl. Phys. Lett. Vol. 74, N°14, pp. 2017-19, 1999.
- [3] M. Jaraiz, L. Pelaz, E. Rubio, J. Barbolla, G. H. Gilmer et al., "Atomistic modeling of point and extended defects in crystalline materials", Mat. Res. Soc. Symp., 1998.
- [4] V. Kaepelin, Z. Chalupa, L. Frioulaud, S. Mehta, B. Guo et al., "Process transferability from a spot beam to a ribbon beam implanter: CMOS device matching", Ion Impl. Tech. Conf. Proc., vol. 866, pp. 353-356, 2006.
- [5] M. D. Giles, "Transient phosphorus diffusion below the amorphization threshold", J. of the Electrochem. Soc., vol. 138, N°4, pp. 1160-65, 1991.
- [6] L. Pelaz, L. A. Marques, G. H. Gilmer, M. Jaraiz, and J. Barbolla: "Atomistic modeling of the effects of dose and implant temperature on dopant diffusion and amorphization in Si", Nucl. Instr. Meth. in Phys. Res. B, vol. 180, pp. 12-16, 2001.
- [7] P. A. Stolk, H.-J. Gossmann, D. J. Eaglesham, D. C. Jacobson, C. S. Rafferty et al., "Physical mechanisms of transient enhanced dopant diffusion in ion-implanted silicon", J. Appl. Phys., vol. 81, N°9, pp. 6031-50, 1997.
- [8] C. Bonafos, A. Claverie, D. Alquier, C. Bergaud, A. Martinez et al., "The effect of the boron doping level on the thermal behaviour of end-of-range defects in silicon", Appl. Phys. Lett., vol 71 N°3, pp. 365-367, 1997.
- [9] N. E. B. Cowern, M. Jaraiz, F. Cristiano, A. Claverie, G. Mannino, "Fundamental diffusion issues for deep-submicron device processing", I.E.D.M. Tech. Dig. Int., pp. 333-336, 1999.